Розділ 3. Інтелектуальні ресурси. Науково-технологічна безпека

УДК 502/504

MODELING OF PHONOELASTIC AND STRAIN-STRESS PROPERTIES OF ^{13}C HIGH PRESSURE SENSOR FOR USE IN ECOLOGICAL SAFETY AND USE OF NATURAL RESOURCES

Andreiy I. Kondrat'yev
(Doctor of Physical and Mathematical Sciences (Mathematical Theory and Applications of Conflict Results Prediction). MS, PhD (Physics) from University of Alabama at Birmingham, USA)

МОДЕЛИРОВАНИЕ НАГРУЗОК-НАПРЯЖЕНИЙ И ФОНОЭЛАСТИЧЕСКИХ СВОЙСТВ ^{13}C-СЕНСОРА ВЫСОКОГО ДАВЛЕНИЯ ДЛЯ ПРИМЕНЕНИЯ В ЭКОЛОГИЧЕСКОЙ БЕЗОПАСНОСТИ И ПРИРОДОПОЛЬЗОВАНИИ

А.И. Кондратьев

We investigate different properties of ^{13}C diamond layer which was grown on a top of a brilliant cut diamond anvil. We connected equations of state for diamond with stress and strain concentrating on the case of [100], see ([1]) strain with diamond anvil bearing load plane as (100), (see [1]). We investigated the behavior of optical Γ phonons with respect to pressure, strain and stress parameters. We also did simulation of these problems using finite element modeling and Nike2D computer software. We used O.H. Nielsen approach for modeling of the sensor.

Досліджуються різноманітні властивості прошарку ^{13}C-алмаза, який виростили на верхівці сенсора-діаманта. Поєднані рівняння стану алмаза

і концентрації з фоноеластичними властивостями. Досліджуються рівняння, які описують поведінку оптичних фонів в термінах тиску і напруги. Проведено моделювання цих проблем з використанням методу кінцевих елементів і програмного забезпечення Nike2D. Для моделювання сенсору було застосовано метод наближення О. Нільсена.

Исследуются различные свойства слоя ^{13}C-алмаза, выращенного на вершине сенсора - бриллианта. Объединены уравнения состояния алмаза и концентрации с фоноэластическими свойствами. Исследуются уравнения, описывающие поведение оптических фононов в терминах давления и напряжения. Проведено моделирование этих проблем, используя метод конечных элементов и программное обеспечение Nike2D. Для моделирования сенсора применен метод приближения О. Нильсена.

Main Hypothesis. We assume that with initial stress and stress and compressing load as (100) the compressive changes in diamond anvils and in high pressure sensor maybe divided in the following consecutive changes:

1. Initial stresses and strains in [100] direction.
2. Stresses and strains in [110] direction.
3. Stresses and strains in [111] direction.

The resultant are elastic and plastic changes in elastic solids and they are mixture of stresses and strains in [100], [110] and [111] directions. As the result the Raman signal will be also the mixture of the signals of strained cells in each of the directions: [100], [110] and [111]. Formally all of these maybe written in the following way.

1. For stress tensor components

$$\vec{\vec{t}} = \alpha_1 \vec{\vec{t}}_{[100]} + \beta_1 \vec{\vec{t}}_{[110]} + \gamma_1 \vec{\vec{t}}_{[111]}; \alpha_1 + \beta_1 + \gamma_1 = 1.$$

2. For strain tensor components

$$\vec{\eta} = \alpha_2 \vec{\eta}_{[100]} + \beta_2 \vec{\eta}_{[110]} + \gamma_2 \eta_{[111]}; \alpha_2 + \beta_2 + \gamma_2 = 1.$$

3. For phonoelastic tensor components

$$\vec{\vec{\Omega}} = \alpha_3 \vec{\vec{\Omega}}_{[100]} + \beta_3 \vec{\vec{\Omega}}_{[110]} + \gamma_3 \Omega_{[111]}; \alpha_3 + \beta_3 + \gamma_3 = 1.$$

Research Goals include investigation, verification, and modeling of Diamond Equations of State, Γ Optical Phonon Behavior, High Pressure Sensor Calibration

Introduction. We study the behavior of Γ optical phonons in diamond anvil which are triply degenerate when strain is not present. When external pressure appears and thus internal strains are present the diamond cubic symmetry does not exist anymore and this triplet is split. On Fig.1 the ^{13}C high pressure sensor is presented.

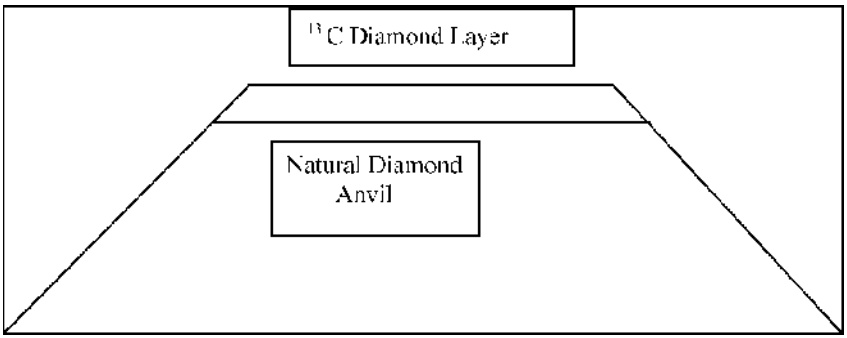

Fig. 1. ^{13}C High Pressure Sensor in the form of a layer on natural diamond anvil.

Real Problem of Raman Peak Shift. While compressing the sensor and anvils in DAC at 156 GPa pressure we've obtained the following shift of the Raman signal (see Fig. 2).The most interesting thing is that the Raman signal from the sensor is widened and at 156 GPa pressure this signal has the width of 21.51 1/cm. The main goal of this article is to try to analyze this phenomenon and to try to develop the physical and mathematical models of it. Our first step is the data analysis. In Table 1 we put all numerical data of this pressure sensor. We analyze all points on the graph in the range from 1542 1/cm to 1563 1/cm and the peaks (graphs) associated with them.

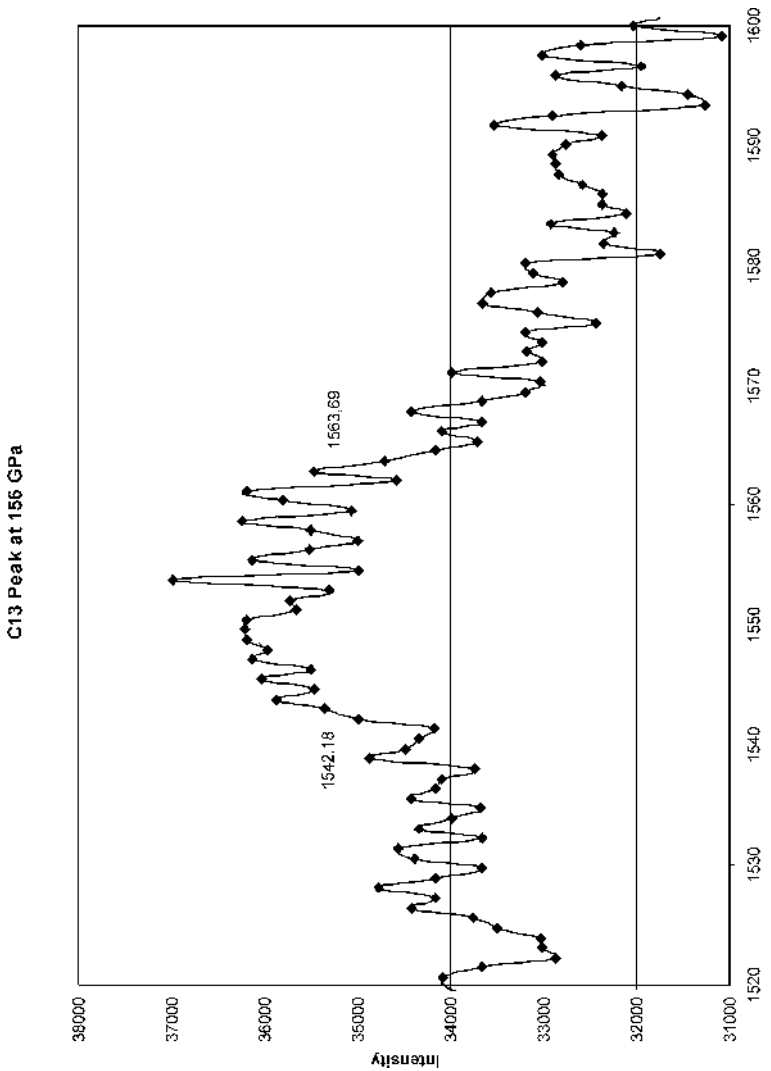

Fig.2. Raman Signal from ^{12}C Natural Diamond Anvils and ^{13}C High Pressure Sensor

Table 1 — **Numerical Presentation of the Raman Signal from High Pressure Sensor**

Number of the Point	Wave Number Value(1/cm)	Intensity of Raman Signal (ye)	Length of the Interval associated with the point (1/cm)
1	1542.18	34977	0.83
2	1543.01	35348	0.82
3	1543.83	35864	0.83
4	1544.66	35472	0.83
5	1545.49	36029	0.83
6	1546.32	35492	0.83
7	1547.15	36133	0.82
8	1547.97	35967	0.82
9	1548.8	36195	0.83
10	1549.63	36216	0.83
11	1550.46	36195	0.82
12	1551.28	35657	0.83
13	1552.11	35719	0.83
14	1552.94	35306	0.83
15	1553.77	36983	0.82
16	1554.59	34977	0.83
17	1555.42	36133	0.83
18	1556.25	35513	0.82
19	1557.07	34997	0.83
20	1557.90	35492	0.83
21	1558.73	36236	0.82
22	1559.55	35059	0.83
23	1560.38	35802	0.83
24	1561.21	36195	0.82
25	1562.03	34586	0.83
26	1562.86	35472	0.83
27	1563.69	34709	0.82

We can see that all relative width for each point signal is about the same as 0.82–0.83 1/cm.

Our next step is to analyze the local peaks which are parts of this part of the curve. These local curves (peaks) are described in Table 2.

Elements of Lagrangian Elastic Theory. There are different ways to present Lagrangian point of view on Solid Mechanics issues. The way the most close to our goals is presented in [1].

Within Lagrangian elastic theory for a strain tensor $\vec{\eta}$ and $\vec{t}$ as a stress tensor we have

$$\vec{\eta} = \vec{\varepsilon} + \frac{1}{2}\vec{\varepsilon}^{\,2},$$

$$\vec{t} = \det(\vec{1} + \vec{\varepsilon})(\vec{1} + \vec{\varepsilon})^{-1}\vec{\sigma}(\vec{1} + \vec{\varepsilon})^{-1}.$$

Table 2 – **Description of the Peaks n the Raman Signal from High Pressure Sensor**

Number of the Peak (Curve)	Points (Vertices) Included in the Peak	Corner Vertices of the Peak	Length of the Peak (1/cm)	Maximum Intensity of the Peak (ye)	Left Boundary (1/cm)	Right Boundary (1/cm)
1	1, 2, 3, 4	1, 4	2.48	36864	1542.18	1544.66
2	4, 5, 6	4, 6	1.66	36029	1544.66	1546.32
3	6, 7, 8	6, 8	1.65	36133	1546.32	1547.97
4	8, 9, 10, 11, 12	8, 12	3.31	36216	1547.97	1551.28
5	12, 13, 14	12, 14	1.66	35719	1551.28	1552.94
6	14, 15, 16	14, 16	1.65	36983	1552.94	1554.59
7	16, 17, 18, 19	16, 19	2.48	36133	1554.59	1557.07
8	19, 20, 21, 22	19, 22	2.48	36236	1557.07	1559.55
9	22, 23, 24, 25	22, 25	2.48	36195	1559.55	1562.03
10	25, 26, 27	25, 27	1.66	35472	1562.03	1563.69

where $\vec{\vec{\varepsilon}}$ is a physical strain tensor defined by the replacement in the following $\vec{r} \to (\vec{\vec{1}} + \vec{\vec{\varepsilon}})\vec{r}$, and $\vec{\vec{\sigma}}$ is a physical stress tensor. General strain-stress relations are

$$t_i = \sum_j C_{ij}\eta_j + \frac{1}{2}\sum_{j,k} C_{ijk}\eta_j\eta_k + \ldots$$

$$\vec{u} = \sum_j A_j\eta_j + \frac{1}{2}\sum_{j,k} A_{jk}\eta_j\eta_k + \ldots,$$

where C_{ij}, C_{ijk} are elastic constants and $\vec{u}$ is a vector of all relative replacements and A_j, A_{jk} are internal strain tensors. We assume that bearing load plane of diamond anvil and bearing load of the **^{13}C** diamond layer to be parallel and to be (100). We have then the case of strain directed as [100] and thus the strain tensor $\vec{\vec{\eta}}$ will be written in rather simple way

$$\vec{\vec{\eta}}_{[100]} = \begin{bmatrix} \eta_1 & 0 & 0 \\ 0 & 0 & 0 \\ 0 & 0 & 0 \end{bmatrix}.$$

Notice that for the case of [110] strain the tensor will be

$$\vec{\vec{\eta}}_{[110]} = \begin{bmatrix} \eta_1 & \eta_1 & 0 \\ \eta_1 & \eta_1 & 0 \\ 0 & 0 & 0 \end{bmatrix}.$$

For the case of [111] case the tensor will look like this

$$\vec{\vec{\eta}}_{[111]} = \begin{bmatrix} \eta_1 & \frac{1}{2}\eta_4 & \frac{1}{2}\eta_4 \\ \frac{1}{2}\eta_4 & \eta_1 & \frac{1}{2}\eta_4 \\ \frac{1}{2}\eta_4 & \frac{1}{2}\eta_4 & \eta_1 \end{bmatrix}.$$

$$t_1 = C_{11}\eta_1 + \frac{1}{2}C_{111}\eta_1^2;$$

$$t_2 = t_3 = C_{12}\eta_1 + \frac{1}{2}C_{112}\eta_1^2$$

For [100] strain case the stress tensor $\vec{\vec{t}}_{[100]} = \begin{bmatrix} t_1 & 0 & 0 \\ 0 & t_2 & 0 \\ 0 & 0 & t_3 \end{bmatrix}$ is presented by the main components t_1, t_2, t_3. In our case they are equal to.

For case of [110] strain case the stress tensor components $\vec{\vec{t}}_{[110]}$ are written in the following way

$$t_1 = t_2 = (C_{11} + C_{12})\eta_1 + \frac{1}{2}(C_{111} + 3C_{112} + 4C_{166})\eta_1^2,$$

$$t_3 = 2C_{12}\eta_1 + (C_{112} + C_{123} + 2C_{144})\eta_1^2,$$

$$t_6 = 2C_{44}\eta_1 + 4C_{166}\eta_1^2.$$

For case of [111] strain case the stress tensor components $\vec{\vec{t}}_{[111]}$ are written in the following way

$$t_1 = t_2 = t_3 = (C_{11} + 2C_{12})\eta_1 + \frac{1}{2}(C_{111} + 6C_{112} + 2C_{123})\eta_1^2 +$$

$$+ \frac{1}{2}(C_{144} + 2C_{166})\eta_4^2,$$

$$t_4 = t_5 = t_6 = C_{44}\eta_4 + (C_{144} + 2C_{166})\eta_1\eta_4 + C_{456}\eta_4^2.$$

We also plan to use Eulerian approach in order to use the Birch equation of state and to compare each obtained result in both theories. Both theories differ in the coordinate systems being fixed and associated with some apriori chosen inertial coordinate system

or coordinate system is being inbuilt in the solid and is under transformation as well as the solid is. We present the Birch's results [3] which connects Eulerian strain $\vec{\vec{\eta}}^{E}$ tensor and Eulerian stress tensor $\vec{\vec{t}}^{E}$

$$\vec{\vec{\eta}}^{E} = \frac{1}{2}[\vec{\vec{1}} - (\vec{\vec{1}} + \vec{\vec{\varepsilon}})^{-2}] = \frac{1}{2}[\vec{\vec{1}} - (\vec{\vec{1}} + 2\vec{\vec{\eta}})^{-1}];$$
$$\vec{\vec{t}}^{E} = \det(\vec{\vec{1}} + \vec{\vec{\varepsilon}})(\vec{\vec{1}} + \vec{\vec{\varepsilon}})\vec{\vec{\sigma}}(\vec{\vec{1}} + \vec{\vec{\varepsilon}}).$$

In Nike2D model we use cylindrical system of coordinates and regular notation is the following for [100] strain case.

$$\sigma_{zz} = \sigma_1,$$
$$\sigma_{rr} = \sigma_2,$$
$$\sigma_{\vartheta\vartheta} = \sigma_3,$$
$$\sigma_2 = \sigma_3$$

where using elastic constants presented in [1] for Lagrangian and Euler theories we write the following stress/strain dependencies for stress tensor for the case of [100] strain.

Lagrangian Approach.

$$t_1 = 1081\eta_1 - 3150\eta_1^2;$$
$$t_2 = t_3 = 125\eta_1 - 400\eta_1^2$$

Eulerian Approach.

$$t_1 = 1081\eta_1 + 2785\eta_1^2;$$
$$t_2 = t_3 = 125\eta_1 - 415\eta_1^2$$

These relations are shown on Fig. 3.

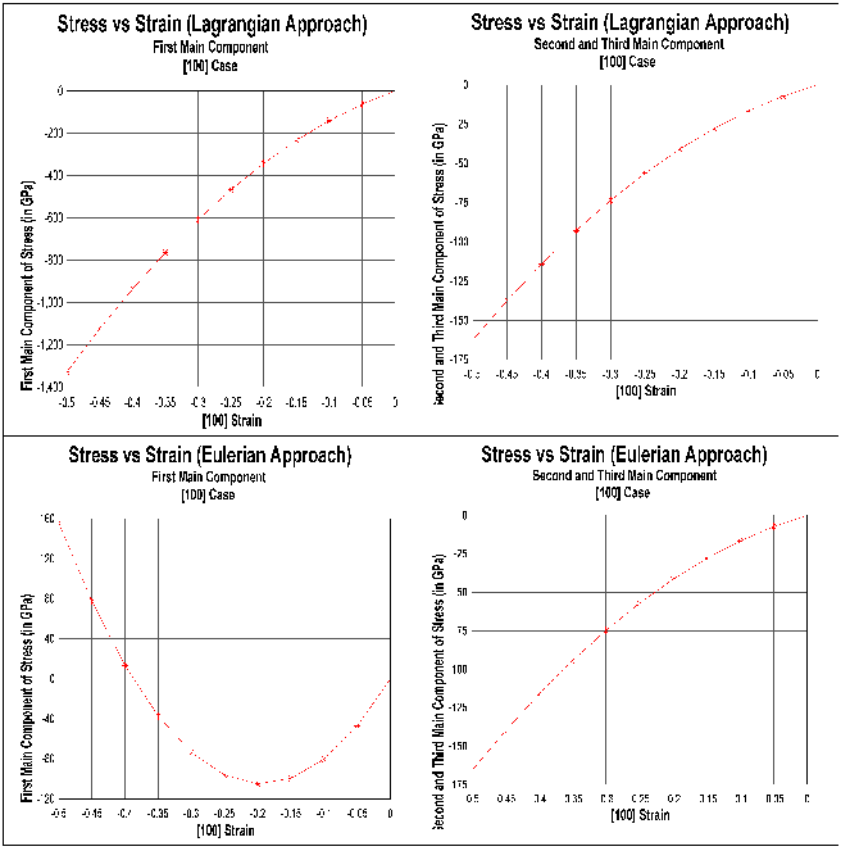

Fig.3. Stress/Strain Relations in Lagrange and Euler theories for [100] strain case

As we can see the Lagrangian approach gives better approximation to the experimental data. Nike2D simulation model also well match First Main Stress Component in the stress tensor for Lagrangian approach. For the case of [110] strain the tensor stress components are

Lagrangian Approach.

$$t_1 = t_2 = 1207\eta_1 - 6450\eta_1^2;$$
$$t_3 = 250\eta_1 - 710\eta_1^2;$$
$$t_6 = 1158.4\eta_1 - 10440\eta_1^2.$$

Eulerian Approach.

$$t_1 = t_2 = 1207\eta_1 + 3103.5\eta_1^2;$$
$$t_3 = 250\eta_1 + 150\eta_1^2;$$
$$t_6 = 1158.4\eta_1 + 3132\eta_1^2.$$

For the case of [111] strain the stress tensor components are. *Lagrangian Approach.*

$$t_1 = t_2 = t_3 = 1331.5\eta_1 - 1875\eta_1^2 - 2595\eta_4^2;$$
$$t_4 = t_5 = t_6 579.2\eta_4 - 5190\eta_1\eta_4 - 1310\eta_4^2.$$

Euleria Approach.

$$t_1 = t_2 = t_3 = 1332.5\eta_1 + 965\eta_1^2 + 859.5\eta_4^2;$$
$$t_4 = t_5 = t_6 = 579.2\eta_4 + 1719\eta_1\eta_4 + 571\eta_4^2.$$

High Pressure Sensor Calibration (Present Models). The use of ^{13}C diamond layer as a high pressure sensor and its calibration was described in [2]. The calibration of this type of sensor was also investigated by different authors and as was confirmed in [2] a quadratic fit for a relative shift of a Raman peak with respect to pressure is a good model. If $\Delta\omega = \omega - \omega_0$ is a relative shift of a Raman peak and P is a pressure then the following quadratic fit $\Delta\omega = aP = bP^2$, where *a* and *b* are constants is valid. Several comparable fits are presented in the Table 3 below.

Diamond Equation of State. We consider two equations of state for diamond : one suggested by Birch [4] , another by Murnaghan [5]. On Fig. (left) the Birch equation of state is shown, on Fig.

Table 3 — **Different Quadratic Fits for a Relative Shift of a Raman Peak**

#	Source	Constant *a*	Constant *b*
1	Eremets	2.258	- 0.0024
2	Akahama et al.	2.179	- 0.0018
3	Sun et al.	2.062	- 0.0014
4	Wei et al.	2.418	- 0.0038
5	Our Nike2D Model	2.423	- 0.0034

(right) the Murnaghan equation of state is shown, on Fig. our Nike2D simulation model results are shown. The Nike2D model simulation results are very close to the Birch model. The parameter used in Nnike2d model is the ratio (V0/V) -1, we use the same parameter for the Birch and Murnaghan models for easy comparison.

If B is a bulk modulus, $B' = \frac{dB}{dP} = \text{constant}$, then for diamond we have the following Murnaghan diamond equation of state.

$$P = 158.62[(\frac{V_0}{V})^{2.9} - 1],$$

V_0 is the volume at ambient pressure and V is a current volume. Birch diamond equation of state

$$P = 658.5\left(\frac{V_0}{V}\right)^{5/3}\left[\left(\frac{V_0}{V}\right)^{2/3} - 1\right]\left[1 + 0.375\left(\left(\frac{V_0}{V}\right)^{2/3} - 1\right)\right]$$

In Nike2D the parameter used is the following ratio: $\left(\frac{V_0}{V}\right) - 1$.

For the purpose of better comparison we present the Birch and Murnaghan equations of state for diamond with respect to the same ratio. Both Birc We notice that much better comparison with Nike2D model diamond equation of state was made for the Birch transformed model. Nike2D model is shown on Fig.5. Birch and Murnaghan transformed functions are shown on Fig.4.

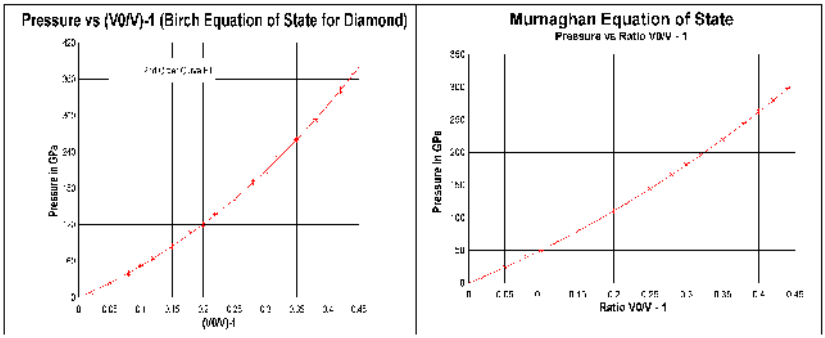

Fig. 4 . Birch transformed and Murnaghan transformed Diamond Equation of State

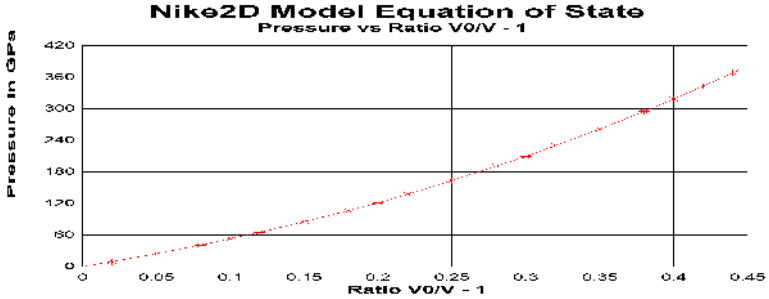

Fig.5. Nike2D Model Diamond Equation of State

Optical Γ Phonon Behavior with respect to Stress and Strain. We assume as in [1] that the optical Γ phonon is completely described by the phonon-frequency tensor

$$\vec{\vec{\Omega}} = \begin{bmatrix} \Omega_1 & \Omega_6 & \Omega_5 \\ \Omega_6 & \Omega_2 & \Omega_4 \\ \Omega_5 & \Omega_4 & \Omega_3 \end{bmatrix}.$$

Phonon-frequency tensor components maybe expressed as functions of strain

$$\Omega_i = \omega_0 \{\delta_i + \sum_j \Omega_{ij}\eta_j + \frac{1}{2}\sum_{j,k}\Omega_{ijk}\eta_j\eta_k + \ldots\},$$

where $\vec{\vec{\delta}} = \{\delta_i\}$ is a unit tensor, $\Omega_{ij}, \Omega_{ijk}$ are dimensionless phonoelastic constants. In the case of [100] strain we have the following relations for normal mode frequencies of phonon-frequency tensor.

$$\Omega_1 = \omega_0(1 + \Omega_{11}\eta_1 + \frac{1}{2}\Omega_{111}\eta_1^2);$$

$$\Omega_2 = \Omega_3 = \omega_0(1 + \Omega_{12}\eta_1 + \frac{1}{2}\Omega_{112}\eta_1^2)$$

Notice that for the case of small pressure value we can restrict our case only with [100] strain. With the pressure increased we have automatically strain appearing in [110] direction and with further pressure increase in [111] direction. The main reason is that the diamond unit cell are being deformed from its initial equilibrium position and those cases will automatically appear due shear stress and other effects.The resultant strain is some linear combination of strains in all these three directions mentioned above. All of this will cause us also to consider these directions as separate and important ones. For the case of [110] strain we have for phonoelastic tensor

$$\Omega_1 = \Omega_2 = \omega_0[1 + (\Omega_{11} + \Omega_{12})\eta_1 + \\ + \frac{1}{2}(\Omega_{111} + 3\Omega_{112} + 4\Omega_{166})\eta_1^2],$$

$$\Omega_3 = \omega_0[1 + 2\Omega_{12}\eta_1 + (\Omega_{112} + \Omega_{123} + 2\Omega_{144})\eta_1^2],$$

$$\Omega_6 = \omega_0(2\Omega_{44}\eta_{11} + 4\Omega_{166}\eta_1^2).$$

The normal modes for the case of [110] strain are $\Omega_1 + \Omega_6; \Omega_1 - \Omega_6; \Omega_3$. For Lagrangian approach we have the following normal modes for [110] strain

$$\Omega_1 + \Omega_6 = 1281 - 5556.978\eta_1 + 2469.768\eta_1^2;$$

$$\Omega_1 - \Omega_6 = 1281 - 120.414\eta_1 + 3105.144\eta_1^2;$$

$$\Omega_3 = 1281 - 1954.806\eta_1 + 9607.5\eta_1^2.$$

Dependence of strain is shown on Fig.6. Normal modes for [110] strain for Eulerian approach

$$\Omega_1 + \Omega_6 = 1281 - 5295.6\eta_1 - 24273\eta_1^2;$$
$$\Omega_1 - \Omega_6 = 1281 - 381.8\eta_1 + 526.4\eta_1^2;$$
$$\Omega_3 = 1281 - 1954.8\eta_1 + 6994.26\eta_1^2.$$

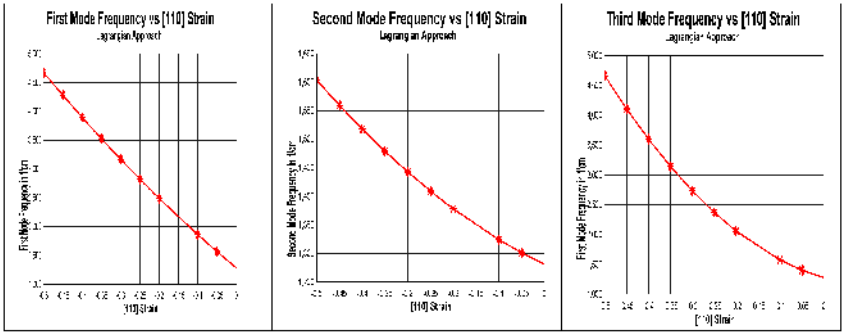

Fig. 6. Normal Modes for Case of [110] Strain (Lagrangian Approach).

On Fig.7 normal modes vs. strain for the case of [110] strain for Eulerian approach is shown.

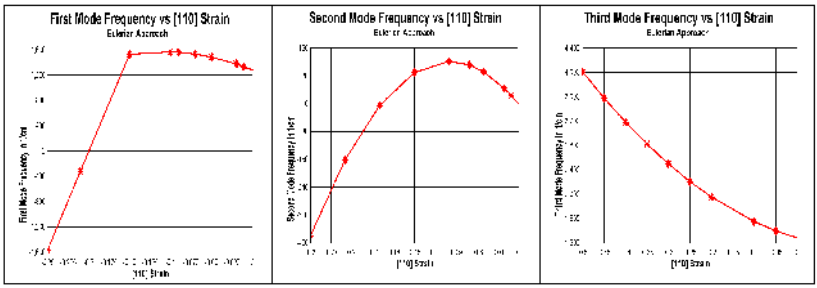

Fig. 7. Normal Modes for Case of [110] *Strain (Eulerian Approach).*

For the case of [111] strain we have the following components of the phonoelastic tensor.

$$\Omega_1 = \Omega_2 = \Omega_3 = \omega_0[1 + (\Omega_{11} + 2\Omega_{12})\eta_1 +$$
$$+ \frac{1}{2}(\Omega_{111} + 6\Omega_{112} + 2\Omega_{123})\eta_1^{\,2} + \frac{1}{2}(\Omega_{144} + 2\Omega_{166})\eta_4^2],$$
$$\Omega_4 = \Omega_5 = \Omega_6 = \omega_0[\Omega_{44}\eta_4 + (\Omega_{144} + 2\Omega_{166})\eta_1\eta_4 + \Omega_{456}\eta_4^2).$$

The normal modes for the case of [111] strain are $\Omega_1 + 2\Omega_4, \Omega_1 - \Omega_4$, the last is double degenerate. The normal modes for the case of [111] strain for Lagrangian approach are

$$\Omega_1 + 2\Omega_4 = 1281 - 3816\eta_1 + 6.885\eta_1^2 -$$
$$- 2449.2\eta_4 + 1537.2\eta_1\eta_4 - 3355.9\eta_4^2;$$
$$\Omega_1 - \Omega_4 = 1281 - 3816\eta_1 + 6.885\eta_1^2 +$$
$$+ 1224.6\eta_4 - 768.6\eta_1\eta_4 + 1678.4\eta_4^2.$$

The normal modes for [111] strain for Eulerian approach are presented in the following way

$$\Omega_1 + 2\Omega_4 = 1281 - 3816\eta_1 - 7107.6\eta_1^2 -$$
$$- 2457\eta_4 - 14014\eta_1\eta_4 - 8653.1\eta_4^2,$$
$$\Omega_1 - \Omega_4 = 1281 - 3816\eta_1 - 7107.6\eta_1^2 +$$
$$+ 1228.5\eta_4 + 7007\eta_1\eta_4 - 928.7\eta_4^2.$$

Our investigation shows that the relative shift of a Raman peak follows the following Hanfland et al [ ] equation. And it is the best fit for it. We have calculated the parameters of Hanfland model fitting experimental data. The model now is

$$P = 859.95\left(\frac{\omega}{\omega_0}\right)^{5/3}\left[\left(\frac{\omega}{\omega_0}\right)^{2/3} - 1\right]\left[1 - 0.2545\left\{\left(\frac{\omega}{\omega_0}\right)^{2/3} - 1\right\}\right].$$

Notice that the parameters of the Hanfland model which fit the experimental data are a = 573.3 GPa, b = 0.2545 (dimensionless). In experimental data we used ω_0 =1281 1/cm. The dependence between ***P* and** ω is shown on Fig. 8. Hanfland dependence is presented in the form of direct and inverse functions. On Fig.9 is shown the same type of dependence we obtained by simulation this problem using the Nike 2D model in the form of direct and inverse functions.

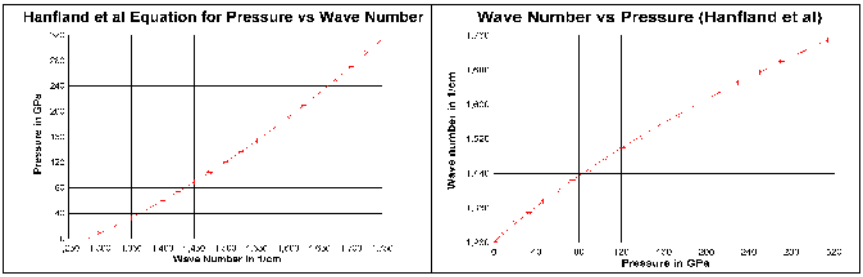

Fig. 8. Hanfland Pressure / Wave Number Model (direct and inverse representation)

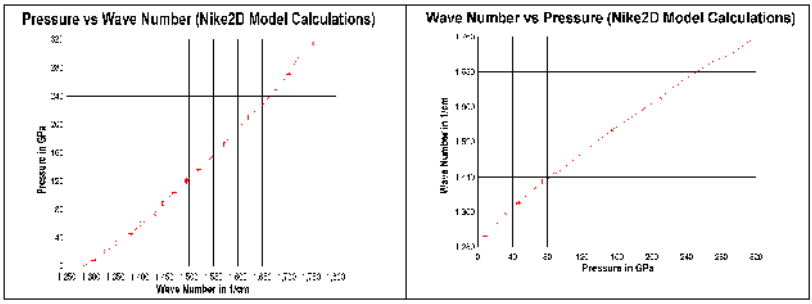

Fig. 9. Nike2d Model connecting pressure and wave number

For alternative model we used Nielsen model [1] which for [100] strain case normal mode frequencies for phonon-frequency tensor will be.

Lagrangian approach.

$$\Omega_1 = 1281 - 1857.45\eta_1;$$

$$\Omega_2 = \Omega_3 = 1281 - 973.56\eta_1 + 960.75\eta_1^2;$$

$$\omega_0 = 1281$$

Eulerian approach.

$$\Omega_1 = 1281 - 1857.45\eta_1 - 3843\eta_1^2;$$

$$\Omega_2 = \Omega_3 = 1281 - 973.56\eta_1 - 832.65\eta_1^2$$

$\omega_0 = 1281$. Both Lagrangian and Euler approaches for Nielsen model are shown on Fig.10.

Maximum Shear Stress. We investigated the behavior of maximum shear stress for [100] strain case in order to find points where the anvil may fail. If $\tau_{\max}$ is a maximum shear stress, then

$$\tau_{\max} = \frac{t_1 - t_2}{2} = \frac{1}{2}\eta_1(C_{11} - C_{12}) + \frac{1}{4}(C_{111} - C_{112})\eta^2$$

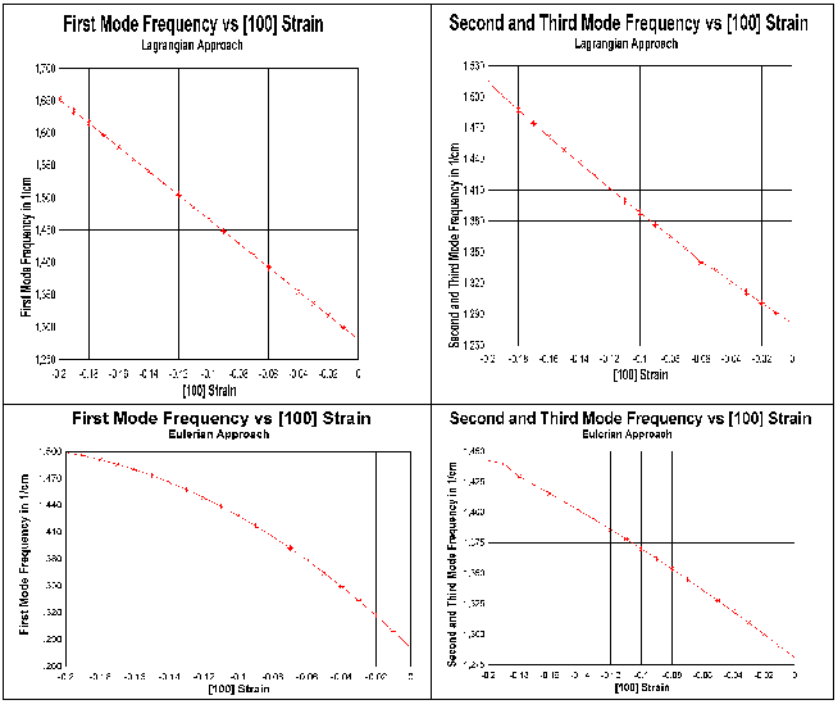

Fig. 10. Normal Mode Frequencies for Nielsen model (Lagrangian and Euler representation)

Lagrangian approach. $\tau_{\max} = 461.5\eta - 1375\eta^2$.

Eulerian approach. $\tau_{\max} = 461.5\eta + 1600\eta^2$.

Both functions are presented on Fig.11. The point of interest for us will be the strain value for which the maximum shear stress reaches value of about 100GPa. Behavior of maximum shear stress is more realistic in Lagrangian approach.

Investigation of *R*1 ratio. We introduce the variable $R1$, $R1 = \dfrac{\sigma_r}{\sigma_z}$

This ratio is rather important in diamond anvil compression problem. Our goal to connect values of $\boldsymbol{R_1}$ with the [100] strain. We have for ratio $R1$

$$R1 = \frac{t_2}{t_1} = \frac{C_{12}\eta_1 + \dfrac{1}{2}C_{112}\eta_1^2}{C_{11}\eta_1 + \dfrac{1}{2}C_{111}\eta_1^2} = \frac{2C_{12} + C_{112}\eta}{2C_{11} + C_{111}\eta}$$

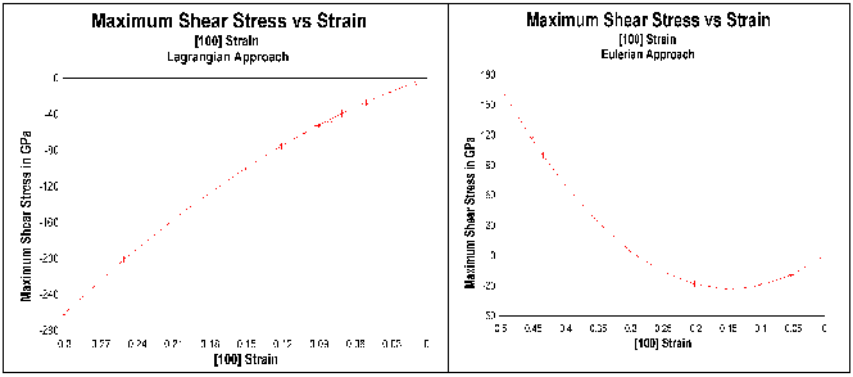

Fig.11. Relation of Maximum Shear Stress vs [100] Strain (Lagrangian and Euler approach).

As the result we obtain.

Lagrangian approach. $R1 = \dfrac{254 - 800\eta_1}{2100 - 6300\eta_1}$.

Eulerian approach. $R1 = \dfrac{254 - 830\eta_1}{2100 + 5570\eta_1}$.

These ratios for Lagrangian and Eulerian approaches are presented on Fig.12. Analysis shows full advantage of Euler theory for $R1$ ratio.

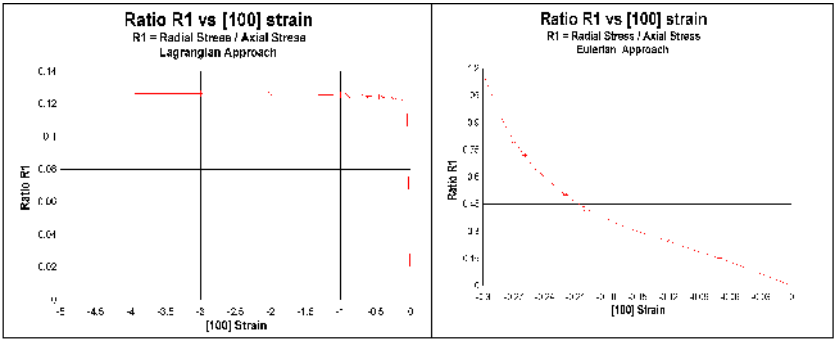

Fig.12. Ratio R1 for Lagrangian and Euler approaches

Description of a Raman Peak Shift of Γ Optical Phonon using Coordinate Position. The advantage of Nielsen model presented before for the case of [100] strain based upon the use of strain tensor component. We connect normal mode frequencies of phonon-frequency tensor with the measuring point location in a strained diamond using $\eta_1 = \dfrac{x}{x_0} - 1$.

Lagrangian approach.

$$\Omega_1 = \omega_0[2.33 - 1.33\frac{x}{x_0}];$$

$$\Omega_2 = \Omega_3 = \omega_0[0.75\left(\frac{x}{x_0}\right)^2 - 2.26\left(\frac{x}{x_0}\right) + 2.51]; \quad \omega_0 = 1281(1/cm)$$

Eulerian approach.

$$\Omega_1 = \omega_0[-3\left(\frac{x}{x_0}\right)^2 + 4.67\left(\frac{x}{x_0}\right) - 0.67];$$

$$\Omega_2 = \Omega_3 = \omega_0[-0.65\left(\frac{x}{x_0}\right)^2 + 0.54\left(\frac{x}{x_0}\right) + 1.11];$$

$\omega_0 = 1281$ 1/cm. These dependencies are presented on Fig. 13.

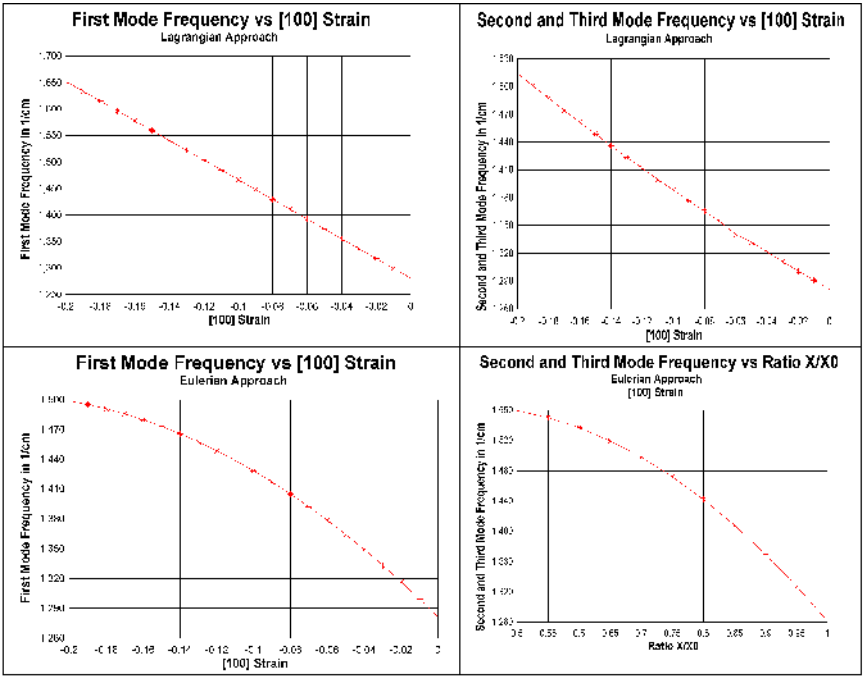

Fig. 13. Normal Mode Frequencies of Optical Γ *Phonon in a* [100] *Strained Diamond*

Notice that both models explain split of triplet of optical phonon in unstrained diamond (Hanfland model does not show that) in a singlet and doublet (First Mode Frequency explains a singlet , the Second and the Third Mode Frequency represent the doublet). Also we can see that these normal modes behavior is relatively close to experimental data (Eulerian approach).

Description of Pressure with respect to Coordinate Position. For the case of [100] strain we don't have any internal parameter to be calculated for describing the internal stress/strain relations. For unstrained diamond for [100] strain case the loading axis is x axis and let x_0 be the initial position. Basically in this case we are talking about the tip of ^{13}C diamond layer, physically it corresponds to the gasket/diamond layer interface. Notice that for the case of $x = x_0$ all stress, strain, pressure values will be equal to zero. By changing the position of x we will obtain stress and strain values not equal zero and for negative values of strain (compression in negative x axis direction) we will connect these values with the stress tensor components. Notice that the same type of curve will be obtained if the pressure on gasket/diamond anvil is not equal zero and lets it will be some value of pressure P_0 , then along the loading axis with respect to loading (axial) coordinate this value will be added to each pressure component. Thus the study of pressure vs coordinate position in a strained diamond is essential. For the strain in [100] direction we have the following relation

$$\eta_1 = \frac{\Delta l}{l_0} = \frac{l - l_0}{l_0} = \frac{l}{l_0} - 1 = \frac{x}{x_0} - 1.$$

Using relation between strain and physical strain tensors can also easily can connect them in the following way:

$\varepsilon_1 = -1 + \sqrt{1 + 2\eta_1}$. We will make the following mathematical assumptions (for the case of [100] strain). $P = \frac{2t_1 + t_3}{3}$, where $t_1 = C_{11}\eta_1 + \frac{1}{2}C_{111}\eta_1^2; t_2 = t_3 = C_{12}\eta_1 + C_{112}\eta_1^2$. Thus

$P = (\frac{2C_{12}}{3} + \frac{C_{11}}{3})\eta_1 + (\frac{C_{112}}{3} + \frac{C_{111}}{6})\eta_1^2$. In the form of pressure/ coordinate x representation

$$P = \left(\frac{x}{x_0}\right)^2 \frac{1}{6}(C_{111} + 2C_{112}) + \left(\frac{x}{x_0}\right)\frac{1}{3}[(C_{11} - C_{111}) +$$

$$+ 2(C_{12} - C_{112})] + \frac{1}{6}[(C_{111} - 2C_{11}) + 2(C_{112} - 2C_{12})].$$

Using elastic constants for Lagrangian and Eulerian theories we obtain the following functions.

Lagrangian approach.

$$P = -1316.67[(\frac{x}{x_0})^2 - 2.33(\frac{x}{x_0}) + 1.33], x \le x_0.$$

Eulerian approach.

$$P = 651.67[(\frac{x}{x_0})^2 - 1.33(\frac{x}{x_0}) + 0.33], x \le x_0.$$

These pressure/loading coordinate relations for Lagrangian and Eulerian approaches are presented on Fig.15. The curve for Lagrangian approach gives a good agreement with our Nike2d computer simulation model.

Change of Total Energy with respect to Strain. We investigate the change of total energy of a diamond using Nielsen approach for [100] strain case. We will have the following function related to strain in [100] direction.

$$\frac{\Delta E_{total}}{V_0} = \frac{1}{2}C_{11}\eta_1^2 + \frac{1}{6}C_{111}\eta_1^3 + \frac{1}{24}C_{1111}\eta_1^4.$$

Using values of elastic constants we obtain

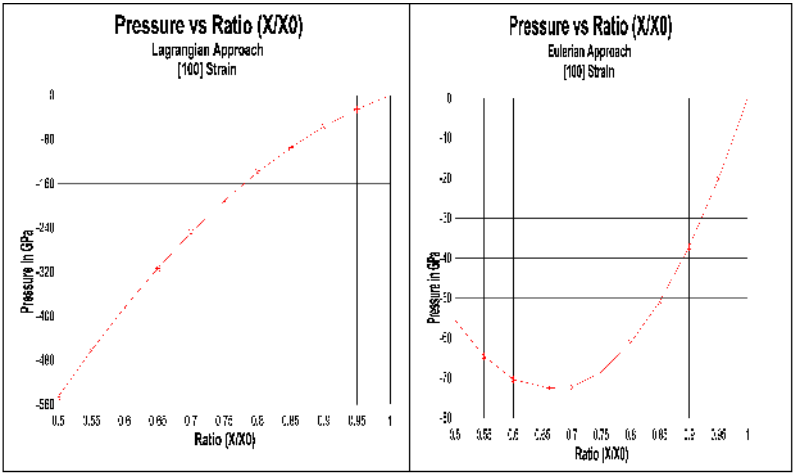

Fig.14. Pressure vs ratio $\frac{x}{x_0}$ *(Lagrangian and Eulerian approach)*

Lagrangian approach. $$\frac{\Delta E_{total}}{V_0} = 525\eta_1^2 - 1050\eta_1^3 + 181.67\eta_1^4 .$$

Eulerian approach. $$\frac{\Delta E_{total}}{V_0} = 525\eta_1^2 + 928.33\eta_1^3 + 679.17\eta_1^4 .$$

Both functions are on Fig. 15.

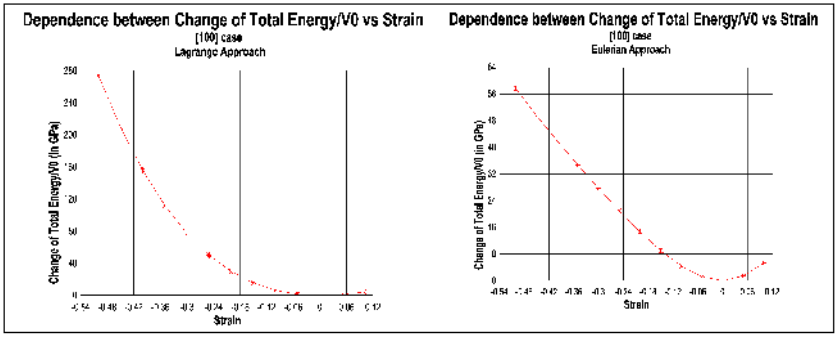

Fig.15. Total Diamond Crystal Energy Change as Function of Strain for [100] case (Lagrangian and Euler Approaches)

Notice that in case of Lagrange approach the energy change is about four times faster than in case of Eulerian approach. On our opinion Lagrangian approach is more preferable.

Conclusions

1. We proved that Hanfland et al model for the relative shift of a Raman peak is a much better fit the the well known and well accepted quadratic fit. The Hanfland model was also confirmed by our simulations on Nike2D computer model.

2. Our Nike2d simulation model has shown the full advantage of Birch equation of state for diamond.

We confirmed by investigation and by computer simulation that under the external pressure the splitting occurs (into singlet and doublet) of Γ 1.optical phonon which was originally triply degenerate in unstrained diamond crystal. Our main results were confirmed in our Nike2D computer simulation model.

2. The peaks 1, 7, 8, 9 (Table 2) are produced by first normal mode in [100] strained compressed sensor cells. Peaks 2, 3, 5, 6, 10 are produced by first normal mode in [110] strained compressed sensor cells. Peak 4 is produced by first normal mode in [111] strained compressed sensor cell.

5. We considered applications of our results in ecological safety and use of natural resources.

Discussion

1. We study the behavior of Γ phonons along the loading axis of diamond anvils and high pressure sensor. While being compressed the strained diamond anvils and high pressure sensor cells along the initial loading axis will be located in arbitrary order with respect to the direction of this axis. For a randomly chosen diamond cell along the Γ phonon axis the direction of a cell axis

$$\vec{n} = (\cos\alpha, \cos\beta, \cos\gamma); \quad \cos^2\alpha + \cos^2\beta + \cos^2\gamma = 1.$$

Then we have the following

$$\begin{pmatrix}\cos\alpha\\ \cos\beta\\ \cos\gamma\end{pmatrix} = \cos\alpha\begin{pmatrix}1\\0\\0\end{pmatrix} + \cos\beta\begin{pmatrix}0\\1\\0\end{pmatrix} + \cos\gamma\begin{pmatrix}0\\0\\1\end{pmatrix} =$$

$$(\cos\alpha - \cos\beta)\begin{pmatrix}1\\0\\0\end{pmatrix} + (\cos\beta - \cos\gamma)\begin{pmatrix}1\\1\\0\end{pmatrix} + \cos\gamma\begin{pmatrix}1\\1\\1\end{pmatrix}.$$

The last shows that arbitrary chosen strained direction maybe represented as the linear combination of [100], [110], and [111] strained directions.

2. We assume that along the Γ phonon line the diamond cells are arbitrary oriented in all of these three directions [100], [110], and [111] in the proportion $a:b:c; a+b+c=1.$

References

1. *O.H.Nielsen*, Phys.Rev. B, 34, 5808 (1986).
2. *Wei Qiu, P.A.Baker, N.Velisavljevic, Y.K.Vohra, S.T.Weir*, J. Appl.Phys. 99,1 (2006).
3. *F.Birch*, Phys.Rev.71, 809 (1947).
4. *F.Birch*, J.Geophys.Res. 57, 227 (1952).
5. *F.D. Murnaghan*, Proc. Natl. Acad. Sci. USA 50, 697 (1944).
6. *M.Hanfland, K.Syassen, S.Fahy, S.G.Louie, and M.L.Cohen*, Phys.Rev. B 31, 6896 (1985).

Отримано: 17.04.2009 р.